Top tether effectiveness during side impacts

Jordan Majstorovic, Julie Bing, Eric Dahle, John Bolte IV & Yun-Seok Kang
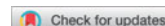
View supplementary material

Published online: 27 Mar 2018.

Submit your article to this journal

View Crossmark data

Taylor & Francis
Taylor & Francis Group

Check for updates

Top tether effectiveness during side impacts

Jordan Majstorovic[a], Julie Bing[a], Eric Dahle[b], John Bolte IV [a], and Yun-Seok Kang [a]

[a]The Ohio State University, Injury Biomechanics Research Center, Columbus, Ohio; [b]Evenflo, Miamisburg, Ohio

ABSTRACT

Objective: Few studies have looked at the effectiveness of the top tether during side impacts. In these studies, limited anthropomorphic test device (ATD) data were collected and/or few side impact scenarios were observed. The goal of this study was to further understand the effects of the top tether on ATD responses and child restraint system (CRS) kinematics during various side impact conditions.

Methods: A series of high-speed near-side and far-side sled tests were performed using the FMVSS213 side impact sled buck and Q3s ATD. Tests were performed at both 10° and 30° impacts with respect to the pure lateral direction. Two child restraints, CRS A and CRS B, were attached to the bench using flexible lower anchors. Each test scenario was performed with the presence and absence of a top tether. Instrumentation recorded Q3s responses and CRS kinematics, and the identical test scenarios with and without a top tether attachment were compared.

Results: For the far-side lateral (10°) and oblique (30°) impacts, top tether attachment increased resultant head accelerations by 8–38% and head injury criterion (HIC_{15}) values by 20–140%. However, the top tether was effective in reducing lateral head excursion by 5–25%. For near-side impacts, the top tether resulted in less than 10% increases in both resultant head acceleration and HIC_{15} in the lateral impact direction. For near-side oblique impacts, the top tether increased HIC_{15} by 17.3% for CRS A and decreased it by 19.5% for CRS B. However, the injury values determined from both impact conditions were below current injury assessment reference values (IARVs). Additionally, the top tether proved beneficial in preventing forward and lateral CRS rotations.

Conclusions: The results show that the effects of the top tether on Q3s responses were dependent on impact type, impact angle, and CRS. Tether attachments that increased head accelerations and HIC_{15} values were generally counterbalanced by a reduction in head excursion and CRS rotation compared to nontethered scenarios.

Introduction

Motor vehicle crashes have remained among the leading causes of serious injury and death for children (Arbogast and Durbin 2013). Side impacts are the second most frequent type of collision and can cause serious head, neck, and chest injuries to pediatric occupants (Arbogast and Durbin 2013; Maltese et al. 2007; Sherwood et al. 2003; Sullivan and Louden 2009). Two side impact modes, near- and far-side impacts, have gained attention in the automotive safety research community. Starnes and Eigen (2002) analyzed passenger vehicle crash data and reported that the number of near-side impact fatalities was 2.6 times greater than the number of far-side fatalities. The increased fatality risk can be attributed to more severe lateral movement of the child and direct loading of the child restraint system (CRS)/occupant by intruding vehicle structures (Fildes et al. 2003; Franklyn et al. 2007; Howard et al. 2004; Klinich et al. 2005). However, significant injuries also occurred with minor or even no intrusion of vehicle structures (Arbogast et al. 2000).

Age-appropriate CRSs have proved an effective way to reduce the risk of injury and death during motor vehicle collisions.

The effectiveness of the CRS comes from its ability to distribute forces over the shoulders and hips of the child, while reducing head and chest excursion (Kahane 1986). Additionally, the implementation of regulations regarding child restraint protection during motor vehicle crashes has further helped reduce the number of child fatalities. National Highway Traffic Safety Administration (NHTSA) has issued a notice of proposed rulemaking (NPRM) to amend FMVSS No. 213 to adopt side impact performance requirements for all CRS designed to seat children up to 40 lb. (NHTSA 2014). The amendment outlines an additional test in which the CRS must protect the child occupant in a dynamic sled test, which simulates a side impact full-scale crash test with door intrusion. The recent attention gained by side impacts has sparked research to focus on various factors affecting child safety during various impact conditions, such as CRS design and its attachment method.

The lower anchors and tethers for children (LATCH) system was developed to standardize the method of attaching child restraints to vehicle seats in an effort to reduce misuse and improper installation resulting from the traditional 3-point seat

Figure 1. Sled set up using Takata side impact bench.

Figure 2. Steel bracket and strap utilized to restrict the sliding seat during far-side sled tests.

belt attachment method (Arbogast and Jermakian 2007). The LATCH anchorage system in vehicles features 3 attachment points: 2 lower anchors and a top tether anchor. The top tether's effectiveness during frontal impacts has been well documented; it has been shown to reduce head excursion, lower neck loads, and reduce chest acceleration (Legault et al. 1997; Lumley 1997). However, less is known about its effects during side impacts. In response, a few studies have looked to understand the top tether's effectiveness in side impact sled tests (Hauschild et al. 2016; Klinich et al. 2005). Klinich et al. (2005) performed a series of far-side impact sled tests to understand the effects of the top tether on lateral head excursion and found a 25- to 100-mm reduction with top tether use. Hauschild et al. (2016) conducted a series of 9 sled tests with a forward-facing CRS on a small sport utility vehicle seat in side impacts to investigate the effects of the top tether in the center seat position on child anthropomorphic test device (ATD) responses. They found that the top tether effectively reduced lateral head excursion from a median of 442 mm without top tether to 400 mm with top tether. Though these studies provide some insight on the effectiveness of the top tether in side impacts, few side impact scenarios were explored.

The main objective of this study was to further understand the effects of the top tether on child ATD responses and CRS kinematics in side impacts. A series of high-speed near-side and far-side impact sled tests under various test conditions was conducted. Two parameters, child restraint and impact angle, were varied. Each test scenario was performed with and without the top tether.

Methods

High-speed near-side and far-side sled tests were conducted with a side impact decelerating sled. Sled and seat acceleration time histories are shown in Figure A1 (see online supplement). A side impact bench seat designed by TK Holdings Inc. (Takata, Auburn Hills, MI) and upgraded by NHTSA was used in this study (Figure 1). The sled buck featured a sliding vehicle seat mounted on a short rail system, along with a side door structure rigidly mounted to the sled buck (Figure 1). The sliding vehicle seat is positioned 250 and 218 mm away from the aluminum honeycomb and the side door structure, respectively (Figure 1). The sled buck travels down a rail system and experiences an abrupt deceleration to simulate near side impacts. The principle of the design was that the sliding vehicle seat slides along the short rail system on the sled buck and impacts the side door
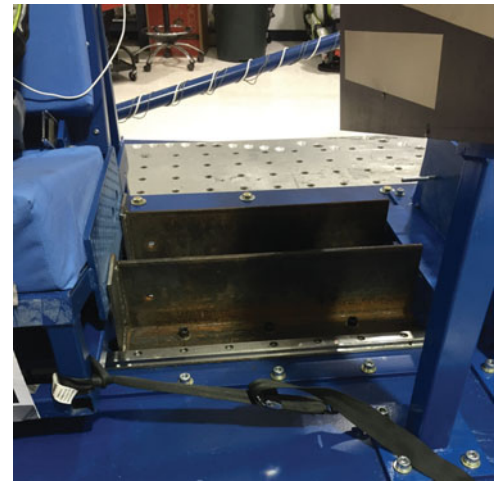
structure. During this contact, the aluminum honeycomb begins to crush, replicating the intrusion velocity of the door that the CRS would experience during an actual vehicle crash (Sullivan and Louden 2009). Further testing procedure details are described in the NPRM amendment document to the FMVSS No. 213 standard (NHTSA 2014). The far-side impacts were performed with a slight modification to the sled test setup. The sliding seat was fixed in place with a steel bracket and a strap to prevent relative movement between the sled buck and seat (Figure 2). Though the sled buck acceleration pulse was comparable for the near-side and far-side sled tests, the seat acceleration pulse for the far-side was different due to the restriction on the sliding seat. As a result, direct comparisons between near-side and far-side sled tests should take this into consideration.

The sled tests were performed with the Q3s ATD (Humanetics, Plymouth, MI). The sled buck was designed such that the sliding vehicle seat could be rotated to simulate different impact angle directions. In this study, the sliding seat was oriented to mimic lateral (10°) and oblique (30°) impact directions (note that a pure lateral side impact was considered 0°). Two forward-facing child restraints were utilized, CRS A and CRS B, and were attached to the sliding vehicle seat using the flexible LATCH system. Each test scenario was performed with and without a top tether attachment, and the top tether anchor was located on the base frame behind the seat as described in FMVSS No. 213 NPRM (NHTSA 2014).

Instrumentation throughout the sled test environment was used to record Q3s and CRS kinematics at 10,000 Hz. High-speed video was recorded from a front camera view at 1,000 frames per second. The Q3s ATD featured 3 accelerometers (Endevco model 7264C 2K, Meggitt Sensing Systems, Irvine, CA) and 3 angular rate sensors (ARS 8K, Diversified Technical Systems, Inc., Seal Beach, CA) located in the head to capture 6 degrees of freedom head kinematics. Head injury criterion (HIC_{15}) values were calculated from the resultant head accelerations. An Infra-Red Telescoping Rod for the Assessment of Chest Compression (IR-TRACC, Humanetics, Plymouth, MI) sensor was located in the Q3s thorax to record lateral chest deflection. For the far-side impact sled tests, an additional 3 accelerometers were added to the thorax to record chest accelerations. The Q3s sensor signals were filtered in accordance
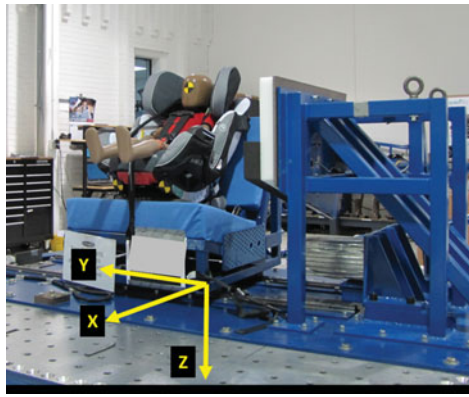
Figure 3. CRS coordinate system.

with the SAE J211 standard (Society of Automotive Engineers 2007). A 3aω motion block composed of 3 accelerometers and 3 ARS was mounted on the far-side base of the child restraint. Data from the motion block were processed and transformed to a coordinate system shown in Figure 3 (Kang et al. 2011). One photo target at the center of the gravity of the Q3s head (Figure 1) was placed to track lateral head motions using video analysis software (TEMA, Image Systems Motion Analysis, Linköping, Sweden). Lateral CRS base motions were quantified by averaging motions from 2 photo targets attached to the CRS bases shown in Figure 1. Table A1 (see online supplement) explains which instrumentation was used for measuring or calculating results from this study.

Results

Near-side impacts

Q3s and CRS kinematics for the lateral and oblique impact directions in the near-side impact sled tests are shown in Figures A2 and A3 (see online supplement), respectively.

Q3s responses

Table 1 displays the peak values for the Q3s responses during the near-side impact sled tests. It should be noted that all values were below current injury assessment reference values (IARVs; Mertz et al. 2016). For the lateral impact direction, the top tether increased the resultant head accelerations by approximately 3–7%. The top tether increased HIC$_{15}$ by 4.4 and 3.3%, for CRS A and CRS B, respectively. For the oblique impacts, the top tether increased resultant head acceleration for CRS A, whereas it decreased it for CRS B. The HIC$_{15}$ values followed the same trend: A 17.3% increase and 19.5% decrease when the top tether was utilized for CRS A and CRS B, respectively. The top tether

did not have a large effect on resultant head angular velocity for CRS A, resulting in less than a 5% difference. For CRS B, the top tether decreased resultant head angular velocity by 11.1% during the lateral impact but increased it by 13.2% during the oblique impact. The Q3s head did not directly impact the door panel in any tests. The Q3s head contacted the interior of the CRS side wing and the exterior of the side wing and main body structure of the CRS impacted the door panel.

Most of the peak chest deflections for the sled tests were relatively small (<8 mm). However, the lateral impact and CRS B scenario produced the following chest deflections: 18.8 mm untethered and 16.0 mm tethered. In this scenario, the top tether reduced the chest compression by 15.1%, resulting in a reduction of 2.8 mm.

CRS kinematics

The CRS rotations for the near-side impacts are shown in Figure 4. For the lateral impact, CRS B, and no top tether test scenario, a problem with one of the CRS ARSs occurred. CRS kinematic data for this scenario were not reported. The top tether reduced x-axis (roll or lateral) CRS rotations; however, all rotations were less than 6°. For the y-axis (pitch or forward/backward) CRS rotations, the lateral impacts produced rotations less than 4°. For the oblique impacts, the top tether reduced the y-axis rotation from 10.2° to 4.1° for CRS A and from 13.5° to 3.2° for CRS B. This was a decrease of 60 and 76% for CRS A and CRS B, respectively.

Relationship among the measured variables

Pearson correlations (R) were examined among the measured variables shown in Table A2 (see online supplement). None of variables exhibited statistical significance and correlation with the exception of resultant head acceleration and HIC$_{15}$ ($P = .001$ and $R = 0.921$).

Far-side impacts

Q3s and CRS kinematics for the lateral and oblique impact directions in the far-side impact sled tests are shown in Figures A3 and A4 (see online supplement), respectively.

Q3s responses

Table 2 displays the peak values for the Q3s responses during the far-side impact sled tests. The top tether increased resultant head accelerations and HIC$_{15}$ values for each test scenario. The percentage increase in resultant head acceleration ranged from approximately 8 to 40%. The percentage increase in HIC$_{15}$ ranged from approximately 20 to 140%. For the oblique impacts,

Table 1. Q3s peak responses from the near-side impact sled tests.

		Lateral (10°)				Oblique (30°)			
		CRS A		CRS B		CRS A		CRS B	
	IARV Mertz et al. (2016)	No tether	Tether	No tether	Tether	No tether	Tether	No tether	Tether
Resultant head acceleration (*g*)	175	70.9	75.6	74.8	77.4	62.5	72.3	67.3	59.2
Resultant head angular velocity (°/s)	N/A	4,549	4,414	3,753	3,337	4,288	4,379	2,850	3,226
Head injury criterion (HIC$_{15}$)	568	435	454	441	455	294	345	333	268
Chest deflection (mm)	23	6.42	4.19	18.8	16.0	7.5	6.6	5.3	7.5

Figure 4. CRS rotations for the near-side sled tests. An asterisk (*) next to the numerical value indicates a negative value defined by the CRS coordinate system (N/A: one ARS was broken during the event).
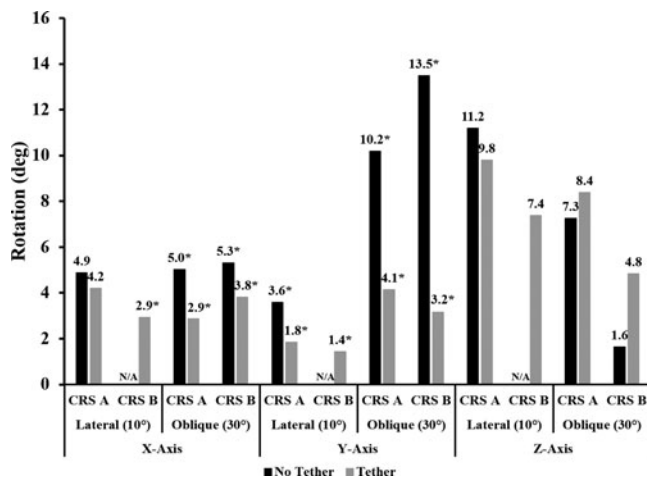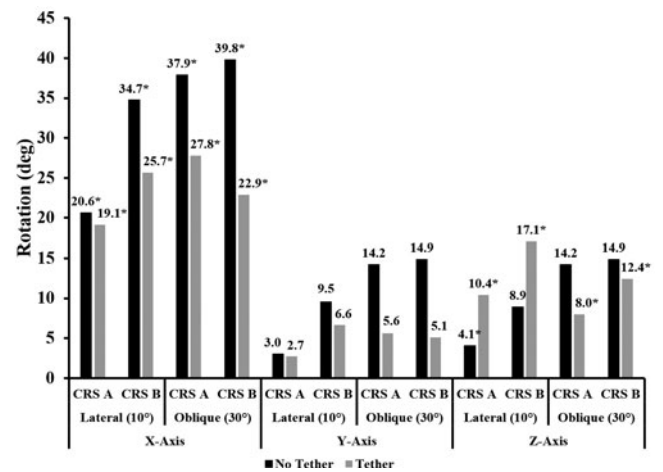

Figure 5. CRS rotations for the far-side sled tests. An asterisk (*) next to the numerical value indicates a negative value defined by the CRS coordinate system.

the top tether increased HIC_{15} by 100.7 and 139.2% for CRS A and CRS B, respectively. HIC_{15} values ranged from 48 to 200. It should be noted that these HIC_{15} values are far below the IARVs shown in Table 2. The top tether decreased lateral head excursion by a range of approximately 5–25% (i.e., 30- to 141-mm reduction). Cross-plots for the resultant head acceleration against the lateral head excursion in the far-side impact tests are shown in Figure A6 (see online supplement).

The top tether increased the resultant chest accelerations during the oblique impacts. The percentage increase was 11.4 and 18.1% for CRS A and CRS B, respectively. However, peak values were lower than the IARV (i.e., 92 g). For the lateral impacts, the top tether reduced the resultant chest acceleration by 10.8% for CRS A and increased it by 41.5% for CRS B. For 3 of the 4 test scenarios, the top tether increased chest deflection by approximately 10–23%. For the lateral impact and CRS B scenario, the top tether reduced chest deflection by 16%.

CRS kinematics

The CRS rotations for the far-side impacts are shown in Figure 5. The top tether effectively reduced x-axis and y-axis CRS rotations. The x-axis (lateral) rotations ranged from 19.1° to 39.8°, and the percentage reductions from top tether usage ranged from approximately 7 to 43%. The y-axis (forward/backward) rotations ranged from 2.7° to 14.9°, and the percentage reductions from top tether usage ranged from approximately 10 to 65%. Patterns for z-axis rotations (yaw) changed depending on impact direction and angle. The lateral CRS base

displacements for the far-side impacts are quantified in Table A3 (see online supplement). At 10° and 30°, respectively, the top tether increased the lateral CRS base displacement by 24.5 and 43.9 mm for CRS A and 49.5 and 74.7 mm for CRS B.

Relationship among the measured variables

Pearson correlations (R) were examined among the measured variables shown in Table A4 (see online supplement). The following variables showed statistical significance and correlation with HIC_{15}: Resultant head acceleration ($P < .001$ and $R = 0.960$), CRS rotation in the x-axis ($P = .015$ and $R = -0.808$), CRS rotation in the y-axis ($P = .011$ and $R = -0.829$), and lateral CRS base displacement ($P = .004$ and $R = 0.883$). However, none of the variables exhibited statistical significance or correlation with the chest deflection.

Discussion

Near-side impacts

The effect of the top tether on Q3s head responses during near-side impacts was dependent on impact angle and CRS (Table 1). During the near-side impact tests, top tether usage resulted in less than 10% increases in resultant head acceleration and HIC_{15} values in the lateral impact direction. During oblique impacts, the percentage differences in resultant head acceleration and HIC_{15} created by top tether usage exceeded 10%. These results suggest that the top tether has a stronger influence on head

Table 2. Q3s peak responses from the far-side impact sled tests.

| | | Lateral (10°) | | | | Oblique (30°) | | | |
| | | CRS A | | CRS B | | CRS A | | CRS B | |
	IARV Mertz et al. (2016)	No tether	Tether	No tether	Tether	No tether	Tether	No tether	Tether
Resultant head acceleration (g)	175	38.6	46.2	37.8	40.9	32.5	40.5	28.2	39.1
Resultant head angular velocity (°/s)	N/A	3,567	3,470	2,722	3,710	2,844	2,931	2,438	2,739
Lateral head excursion (mm)	N/A	508	478	542	408	572	506	595	454
Head injury criterion (HIC_{15})	568	106	200	101	122	66	133	48	114
Chest deflection (mm)	23	10.1	12.6	8.8	7.4	12.9	14.3	12.4	13.8
Resultant chest acceleration (g)	92	50.2	44.8	27.4	38.8	35.9	39.9	31.0	36.6

acceleration and HIC$_{15}$ during near-side impacts in the oblique direction than in the lateral direction. For 3 of the 4 scenarios, when the top tether increased either the resultant head acceleration or resultant head angular velocity, the other decreased (Table 1). This is an interesting finding to consider when trying to mitigate head injury; however, the values were below current IARVs suggested by Mertz et al. (2016). For CRS A, top tether usage resulted in less than a 5% difference for the resultant head angular velocity. For CRS B, the percentage differences ranged from approximately 11 to 13%. The differences in the top tether effect for each CRS can be attributed to individual designs. The CRS B has side wings that are designed to provide extra padding for the whole body during side impacts (shown in Figure A7, see online supplement), whereas these are absent for CRS A (Figures A2–A5, see online supplement).

The maximum chest deflections were in tension (i.e., negative chest deflection) along the lateral axis in the oblique impacts. High-speed video revealed the Q3s rotating during impact and impacting the CRS at an oblique angle from the back. This coupled with the forces from the harness made the thorax bulge out laterally and was believed to cause the negative chest deflection.

The top tether reduced lateral (x-axis) CRS rotation; however, the reduction was less than 3° (Figure 4). This was attributed to the side door interaction during the near-side impacts, which restricted CRS movement. The top tether also reduced forward/backward (y-axis) rotation, with greater reductions during the oblique impact trials (e.g., 6° reduction for CRS A and 10° reduction for CRS B). Differences in the CRS angular kinematics are likely due to different CRS designs, such as different top tether attachments to the CRS (Figure A8, see online supplement), different CRS base shapes (Figure A9, see online supplement), different CRS mass properties, and different structural properties. The top tether proves effective in reducing lateral and forward/backward rotations.

The resultant head acceleration was correlated to the HIC$_{15}$ ($P = .001$ and $R = 0.921$), because HIC$_{15}$ is a function of head acceleration. None of the other measured variables had statistical significance to HIC$_{15}$ or chest deflection in the near-side impacts.

Far-side impacts

A trade-off between resultant head acceleration/HIC$_{15}$ and lateral head excursion was observed during the far-side impacts. The top tether tended to increase Q3s head acceleration, angular velocity, and HIC$_{15}$ during far-side impacts; however, these values were far below current IARVs (Mertz et al. 2016; NHTSA 2014) because the CRS did not impact any interior structures (i.e., no direct loads applied to the CRS). The Q3s did not contact any vehicle structures during the far-side tests, which kept the head injury metrics lower. The top tether proved effective in reducing lateral head excursion during far side impacts (Table 2), which supports the findings from Klinich et al. (2005) and Hauschild et al. (2016). The ability of the top tether to reduce head excursion and CRS rotation is an important benefit. Head and face injuries due to contact against vehicle structures are among the most frequent types of injury sustained by children in forward-facing CRS (Arbogast et al. 2002, 2005). Research suggests that the risk of head and face injuries may increase when CRS attachment to the vehicle is loose (Arbogast et al. 2002) and when the CRS is allowed to rotate toward the point of impact (Arbogast et al. 2005). The top tether offers an additional attachment point to the vehicle frame and, in the current study, appears to reduce lateral head excursion and prevent rotation of the CRS in the vehicle seat. These effects were most obvious in far-side and oblique impacts, which is similar to the findings of Hauschild et al. (2016). With injury metrics for head acceleration and HIC$_{15}$ far below their IARVs for these tests, a small increase in these parameters may be worth the reduction in head excursion and CRS rotation offered by the tether in far-side impacts.

For the oblique impacts, the maximum chest deflections were also in tension (i.e., lateral chest bulge out) along the lateral axis. This is due to anterior-to-posterior compression of the chest in the oblique impacts. The chest instrumentation of the Q3s, IRTRACC, needs to be upgraded so that 2D chest deflection can be captured in the oblique impacts.

The top tether reduced lateral (x-axis) CRS rotation and forward/backward (y-axis) rotation for far-side impacts, with greater reductions during the oblique impact trials (Figure 5). CRS B exhibited better top tether effectiveness on the lateral rotation of the CRS than CRS A. This could be explained by the top tether attachment to the CRS shown in Figure A8. The top tether can slide between the CRS plastic shell and interior foam shown in Figure A8a, whereas the sliding motion was restricted in CRS B (Figure A8b). CRS B showed greater lateral rotation (x-axis) than CRS A, which is likely due to the difference in CRS base shape and size (Figure A9). The back portion of the CRS B base (27.5 cm) is 10 cm narrower than that of the CRS A base (37.5 cm) shown in Figure A9. The narrow base can possibly create more lateral rotation, especially without top tether use, which can explain the differences in CRS rotations in this study (Figure 5). The top tether had a different effect on the z-axis rotation for the lateral and oblique impacts: The top tether reduced z-axis rotation for the oblique impacts and increased it for the lateral impacts (Figure 5). In the lateral impacts, the top tether created a pivot point for the CRS z-axis rotation, which caused greater rotation than the no-tether condition. In the oblique impacts, the top tether effectively reduced the CRS z-axis rotation as well as the x- and y-axis rotations for both CRS A and B. The base displacement in the lateral direction showed an opposite trend compared to the rotational motions. The top tether increased the lateral CRS base displacement for both lateral and oblique directions and for both CRS A and CRS B. Without the top tether, the lower anchors acted as main pivot points while the top portion of the CRS was free to move more laterally. However, with the top tether attached, the top portion of the CRS acted as a main pivot point while the base of the CRS moved more laterally. Thus, lateral base displacements were greater with the top tether attached.

The resultant head acceleration was correlated to the HIC$_{15}$ ($P < .001$ and $R = 0.960$), due to the definition of the HIC$_{15}$ equation (i.e., HIC is a function of head acceleration). The CRS x- and y-axis rotations showed negative correlations with the HIC$_{15}$, which indicates that there is a trade-off between HIC$_{15}$ and CRS rotations in x- and y-axes. The lateral CRS base displacement exhibited statistical significance and positive correlation to the HIC$_{15}$ ($P = .004$ and $R = 0.883$) because the top

tether tended to increase both HIC_{15} and lateral CRS base displacement in the far-side tests.

In order to investigate the role of head protection features such as side wings and energy-absorbing structures, the resultant head acceleration was plotted against the lateral head excursion (Figure A6). The resultant head acceleration measured from CRS B was smaller than that from CRS A regardless of top tether use. Additionally, the reduction in head excursion from CRS B was greater than that from CRS A, likely due to the head protection features of CRS B.

Limitations

A limitation of this study was the Takata sled buck's representation of an actual vehicle-to-vehicle side impact. The side door does not accurately represent individual side door designs with respect to geometry and unique structures. In addition, the bench seat does not accurately represent the contour, bolsters, stiffness, and support structures of an actual rear vehicle seat. Individual vehicle design features, regarding vehicle seats and side doors, may have effects on pediatric occupant responses during side impact crashes. To quantify some of these effects, NHTSA conducted a series of FMVSS No. 214 moving deformable barrier tests with a 2008 Nissan Sentra and 2008 Nissan Versa using a Q3s ATD and 2 CRS models (Sullivan and Louden 2009). The HIC_{15} and chest deflections were slightly higher in the sled tests than in the actual vehicle tests. The Takata sled buck does not capture vehicle design differences; therefore, Q3s and CRS responses may show noticeable differences on actual vehicle seats. This is a standard limitation of a vehicle crash simulator and is often a trade-off to achieve high test repeatability (Sullivan and Louden 2009). However, the lateral head excursion values determined from CRS B with a top tether in the current study (408 mm in the lateral impacts and 454 mm in the oblique impacts) were close to those found in Hauschild et al. (2015), which used the same sled pulse and same CRS B but 20° oblique far-side impacts. They found that the average head lateral excursion from a bench type of vehicle seats was 475 mm, whereas that from a bucket-type vehicle seat was 392 mm.

An additional high-speed camera that captured top view of the ATD head motion was used in this study; however, a video analysis could not be performed for the top view due to issues with the field of view. A lateral view from the high-speed camera was not used in this study, so displacement of the CRS and ATD in the x-axis could not be quantified. Information from a lateral high-speed camera could help us better understand the CRS and ATD performance because the top tether restrains forward motions of the CRS and ATD, especially in the oblique impact condition.

The findings in this study provide insight on the top tether during side impacts for various types of impact scenarios. This information could be valuable for CRS manufacturers to design child restraints that will effectively use the top tether in an effort to reduce injury risk. It is important that the top tether does not cause further injuries during side impacts, because utilization of this mechanism is typically encouraged by CRS manufacturers.

This study performed one sled test for each side impact scenario and it is recommended to continue this research and perform multiple sled tests for each test condition. This will allow for a more accurate understanding of Q3s and CRS responses for each respective test condition, because average values may be calculated and statistical analyses completed. This can be achieved due to the high repeatability of the Takata sled test. However, from this study, repeatability of the test series could not be checked due to the limited number of tests and single sled test per each test condition. Hauschild et al. (2015, 2016) present data for repeated tests in experimental conditions that are similar to those discussed here. The percentage differences in these repeated tests are compared to the responses from the current study under various conditions (e.g., HIC_{15} and lateral head excursion; Figures A10 and A11, see online supplement). The percentage differences between different conditions in the current study were higher than the percentage differences obtained from Hauschild et al. (2015, 2016) repeated studies (Figures A10 and A11). This may indicate that the response differences due to top tether uses from the current study were greater than variations due to repeatability of the experimental conditions. However, caution should be made in interpreting this analysis because experimental setups are not same across studies.

Additionally, it is recommended to investigate the effects of top tether location on top tether effectiveness. Because top tether location varies between each make, model, and year of a vehicle, it may be valuable information for vehicle manufactures to understand which location offers the best CRS performance in side impacts.

ORCID

John Bolte IV http://orcid.org/0000-0001-8301-5547
Yun-Seok Kang http://orcid.org/0000-0002-4730-9908

References

Arbogast KB, Cornejo RA, Kallan MJ, Winston FK, Durbin DR. Injuries to children in forward facing child restraints. *Annu Proc Assoc Adv Automot Med*. 2002;46:213–230.

Arbogast KB, Durbin DR. Epidemiology of child motor vehicle crash injuries and fatalities. In: Crandall JR, Myers BS, Meaney DF, Zellers Schmidtke S, eds. *Pediatric Injury Biomechanics: Archive & Textbook*. New York, NY: Springer; 2013:33–86.

Arbogast KB, Ghati Y, Menon RA, Tylko S, Tamborra N, Morgan RM. Field investigation of child restraints in side impact crashes. *Traffic Inj Prev*. 2005;6:351–360.

Arbogast KB, Jermakian JS. Field use patterns and performance of child restraints secured by lower anchors and tethers for children (LATCH). *Accid Anal Prev*. 2007;39:530–535.

Arbogast KB, Moll EK, Morris SD, Anderko RL, Durbin DR, Winston FK. Factors influencing pediatric injury in side impact collisions. *Annu Proc Assoc Adv Automot Med.* 2000;44:407–428.

Fildes A, Charlton J, Fitzharris M, Langwieder K, Hummel T. Injuries to children in child restraints. *Int J Crashworthiness.* 2003;8: 277–284.

Franklyn M, Peiris S, Huber C, Yang KH. Pediatric material properties: a review of human child and animal surrogates. *Crit Rev Biomed Eng.* 2007;35(3–4):197–342.

Hauschild HW, Humm JR, Pintar FA, et al. The influence of enhanced side impact protection on kinematics and injury measures of far- or center seated children in forward-facing child restraints. *Traffic Inj Prev.* 2015;16(Suppl 2):S9–S15.

Hauschild HW, Humm JR, Pintar FA, et al. Protection of children in forward-facing child restraint systems during oblique side impact sled tests: intrusion and tether effects. *Traffic Inj Prev.* 2016;17(Suppl 1):156–162.

Howard A, Rothman L, McKeag A. Children in side impact motor vehicle crashes: seating positions and injury mechanisms. *J Trauma.* 2004;56:1276–1285.

Kahane CJ. *An Evaluation of Child Passenger Safety: The Effectiveness and Benefits of Safety Seats.* Washington, DC: Department of Transportation; 1986. DOT HS 806 890.

Kang YS, Moorhouse K, Bolte JH. Measurement of six degrees of freedom head kinematics in impact conditions employing six accelerometers and three angular rate sensors (6aω configuration). *J Biomech Eng.* 2011;133:111007.

Klinich KD, Ritchie NL, Manary MA, Reed MP, Tamborra N, Schneider LW. Kinematics of the Q3S ATD in a child restraint under far-side impact loading. Paper presented at: International Technical Conference on the Enhanced Safety of Vehicles; June 6–9, 2005; Washington, DC.

Legault F, Gardner B, Vincent A. The effect of top tether strap configurations on child restraint performance. Paper presented at: 41st Stapp Car Crash Conference; November 12, 1997; Lake Buena Vista, FL.

Lumley M. Child restraint tether straps—a simple method of increasing safety for children. Paper presented at: 41st Stapp Car Crash Conference; November 12, 1997; Lake Buena Vista, FL.

Maltese MR, Locey CM, Jermakian JS, Nance ML, Arbogast KB. Injury causation scenarios in belt-restrained nearside child occupants. *Stapp Car Crash J.* 2007;51:299–311.

Mertz HJ, Irwin AL, Prasad P. Biomechanical and scaling basis for frontal and side impact injury assessment reference values. *Stapp Car Crash J.* 2016;60:625–657.

NHTSA. *Notice of Proposed Rulemaking. 49CFR Part 571. Federal Motor Vehicle Safety Standards; FMVSS 213: Child Restraint Systems—Side Impact Protection.* Washington, DC: 2014. Docket No. NHTSA-2014-0012.

Sherwood CP, Ferguson SA, Crandall JR. Factors leading to crash fatalities to children in child restraints. *Annu Proc Assoc Adv Automot Med.* 2003;47:343–359.

Society of Automotive Engineers. *Instrumentation for Impact Test, Part 1: Electronic Instrumentation.* Author; 2007. SAE J211/1.

Starnes M, Eigen AM. *Fatalities and Injuries to 0–8 Year Old Passenger Vehicle Occupants Based on Impact Attributes.* Washington, DC: Department of Transportation; 2002. DOT HS 809 410.

Sullivan LK, Louden AE. NHTSA's initial evaluation of child side impact test procedures. Paper presented at: International Technical Conference on Enhanced Safety of Vehicles (ESV); June 15–18, 2009; Stuttgart, Germany.